Bio-sorption of ammonium ions by dried red marine algae (*Gracilaria persica*): Application of response surface methodology

Jafari A.[1]; Keramat Amirkolaie A.[1*]; Oraji H.[1]; Kousha M.[1]

Abstract

The bio-sorption of ammonium ions using red marine macroalga *Gracilaria persica* were investigated by response surface methodology. The sorbent was characterized by SEM and FTIR analysis. The influence of various operating parameters such as ammonium concentration (mg L^{-1}), initial solution pH and alga biomass dosage (g L^{-1}) was optimized using Box–Behnken design. A second-order polynomial model successfully described the effects of independent variables on the ammonium ions removal. At the optimum conditions, the maximum removal efficiency was achieved at 100.01 %. The kinetic results also demonstrated that the bio-sorption of ammonium ions by the dried microalga followed well pseudo-second-order kinetics. FTIR results showed that amide, aliphatic and carbonyl groups might be responsible for the adsorption of ammonium ions in aqueous solution by dried *G. persica* biomass.

Keywords: *Gracilaria persica,* Biosorption, Ammonium, Response surface methodology

1-Department of Fisheries, Faculty of Animal Science and Fisheries, Sari Agricultural and Natural Resources University, Sari, Iran

* Corresponding author's Email: amirkola@yahoo.com

Introduction

Developing of different industries is necessary for supporting the needs of growing human population. On the other hand, the increased industrial and agricultural activities have resulted in environmental pollution. In addition, the large amount of water used in our daily life and pollution of natural water resources are the major problems of industrial activities (Deniz and Saygideger, 2011).

There are different types of organic and inorganic contaminants in wastewater, including domestic, agricultural and industrial effluents and contain heavy metals, dyes, phosphorus (P) and nitrogen (N). Over-enrichment of agricultural nutrient sources, particularly P and N in freshwater, can lead to excessive growth of algae in aquatic ecosystems. Transporting of these elements from agricultural lands and aquaculture farms to aquatic systems can result in algal blooms, with the subsequent eutrophication of rivers and lakes after cell death and microbial decay (Galloway *et al.,* 2004; Neal and Heathwaite, 2005).

The ammonium ion (NH_4^+) is generated when ammonia (NH_3) is dissolved in water. The main sources of ammonium nitrogen, which releases into the natural waters such as lakes, rivers and enclosed coastal areas, are synthetic fertilizers, aquaculture wastewater, municipal wastewater, detergent manufacturing and mineral processing industries (Wahab *et al.,* 2012). Among the inorganic pollutants in aquatic ecosystems, the excessive ammonium ion can cause the eutrophication, depletion of dissolved oxygen and obvious toxicity to fish and other aquatic organisms (Liu *et al.,* 2010). Therefore, discovering low-cost and effective techniques to reduce or eliminate ammonium nitrogen from natural water bodies is crucial. Several treatment processes including biological, physical and chemical methods or a combination of them have being employed for the removal of ammonium from wastewater. Adsorption, chemical precipitation, membrane filtration, reverse osmosis, ion exchange, air stripping, breakpoint chlorination, biological nitrification and denitrification are widely used for this purpose (Zheng *et al.,* 2008). However, there are some disadvantages such as low efficiency, long equilibrium time and cost operation for conventional wastewater treatment technologies (Fan *et al.,* 2012). Among the numerous techniques used for wastewater treatment, biosorption method is more economically feasible and environmentally friendly.

Several inexpensive, commonly available, effective and easily obtainable natural and mineral materials, such as bagasse fly ash, olive stone, marine sediment, clay, hazelnut shells, moss, zeolites, limestone, carbon nano-tubes, sawdust, fly ash, red mud, marine algae and seashells have been reported as some types of adsorbents (Kismir and Aroguz, 2011). Marine algae are popular bio-adsorbents for wastewater treatment. They are biological resources with high sorption capacity that are widely available in natural environment. There is a high capacity to retain pollutants by some functional groups contains hydroxyl, carboxyl, amino, sulfhydryl, and sulfonate groups in the algae (Davis *et al.,* 2003).

There are many studies on biosorption of heavy metals and dyes molecules using marine macroalgae, however their efficiency in inorganic pollutants removal is often questionable. The objective of this study was to examine the feasibility of using a red marine macroalgae, *Gracilaria persica*, as a bio-adsorbent of ammonium from aqueous solutions. Initially, efforts were made to optimize the effects of alga dose, initial ammonium concentration and initial solution pH by applying Box–Behnken design under response surface methodology. The mechanism of ammonium biosorption was elucidated using SEM and FTIR results.

Material and methods
Chemicals
Analytical grade ammonium chloride salt (NH_4Cl) and distilled water were used for the preparation of an ammonium stock solution at 10 mg L^{-1} concentration. The other solutions of ammonium were prepared by serial dilution stock solution with distilled water.

Biomass preparation
The red macroalgae, *G. persica*, were collected from the Oman Sea, coast of Chabahar, Iran. The harvested fresh macroalgae were rinsed with tap water and washed several times with distilled water to remove extraneous materials and salt. The biomass was sun dried for three days and then dried in an oven at 70 ^{o}C for 24 h. The dried algae biomass was cut and sieved and the particles size range from 160 to 250 μm were used for the experiments.

Batch experiments
Batch experiments designed by RSM were carried out using 100 ml conical flasks containing 50 ml of the test solutions at the desired initial concentration. The effect of pH on the sorption percent was evaluated in the initial solution pH range of 3, 6 and 9. The pH was measured by a digital pH meter (Sartorius pH meter PB-11, USA) and adjusted by adding 0.1 M HCl and NaOH solutions. The dried algae in the range of 0.5, 1 and 1.5 g L^{-1} was used to examine the effects of biomass dosage on ammonium sorption. The mixtures were shaken using a platform shaker (Dragon LAB, SK- 330- pro, Germany) at 130 rpm and 27 °C to reach equilibrium. The resulting solutions were filtered through 0.2 mm membrane filters (Orange Scientific, GyroDisc CA-PC, Belgium). The residual ammonium concentration was analyzed by the Standard Methods of Examination of Water and Wastewater (Rice *et al.,* 2012), using an UV-VIS spectrophotometer (Hach, DR/2800, USA).

The yield of ammonium removal (*Y*, %) was determined as the percentage of sorbate removed with respect to its initial amount:

$$Y(\%) = \frac{C_i - C_f}{C_i} \times 100 \qquad \text{eq. (1)}$$

Where, C_i and C_f were the concentrations of ammonium (mg L^{-1}) at the beginning of the run and after a given time.

Experimental design
Box-Behnken Design, which is well suited for fitting a quadratic surface and usually works well for the process optimization, was used for the experimental design (Wahab *et al.,* 2010; Wahab *et al.,* 2012).

Therefore, three process variables, namely, initial ammonium concentration (0.5, 2 and 3.5 mg L^{-1}), initial solution pH (3, 6 and 9) and biomass dosage (0.5, 1 and 1.5 mg L^{-1}) were chosen. Totally, 18 experiments were designed by Design Expert software (Version 8.0.4, Stat-Ease, Inc., Minneapolis, United States) statistical package. The coded values (*x*) of process variables were found from Eq. 2 (Kousha *et al.*, 2013):

$$x = \frac{x_i - x_0}{\Delta x} \qquad \text{eq. (2)}$$

Where, $i = 1, 2, 3, \ldots$, x_i is the dimensionless value of a process variable, x_o is the value of x_i at the center point, and Δx is the step change. A second-order model was used to fit the quadratic equation (Kousha *et al.*, 2013):

$$Y = \beta_o + \beta_1 x_1 + \beta_2 x_2 + \beta_3 x_3 + \beta_{12} x_1 x_2 + \beta_{13} x_1 x_3 + \beta_{23} x_2 x_3 + \beta_{11} x_1^2 + \beta_{22} x_2^2 + \beta_{33} x_3^2$$
eq. (3)

where, Y is the measured response (ammonium removal efficiency, %), x_1, x_2 and x_3, are the coded input variables, β_o is the intercept term, β_1, β_2, and β_3 are the linear coefficients showing the linear effects, β_{12}, β_{13} and β_{23} are the cross-product coefficients showing the interaction effects of four process variables, and β_{11}, β_{22} and β_{33} are the quadratic coefficients.

Sorption Kinetics
Kinetics studies were conducted on a platform shaker with a shaking speed of 130 rpm at 27 °C. A concentration of 3.5 mg L^{-1} of the ammonium solution was used for the kinetic studies. 0.5 g L^{-1} of the algal biomass was added into 250 ml of the solution taken in a 500 ml beaker. At time zero and pre-defined time intervals, 5 ml of the solution was taken-out of the beaker and filtered. The amount of dye

adsorbed at a particular time interval was calculated by using the equation 1. Three kinetic models, viz., pseudo-first order, pseudo-second order, and intra-particle diffusion models, were used to understand the sorption kinetics.

The linear form of pseudo-first-order rate expression of Lagergren is given as (Lagergren, 1898):

$$\log(q_e - q_t) = \log q_e - \frac{k_1}{2.303} . t \qquad \text{eq. (4)}$$

Where, q_e and qt are the amounts of dye adsorbed on the adsorbent (mg g^{-1}) at equilibrium and at time t (min), respectively, and k_1 is the rate constant of pseudo-first-order kinetics.

Data was also examined by the pseudo-second order kinetic model shown below (Ho and McKay, 1999) :

$$\frac{t}{q_t} = \frac{1}{k_s q_e^2} + \frac{1}{q_e} t \qquad \text{eq. (5)}$$

Where, qe and qt have the same meaning as mentioned previously, and k_s is the rate constant for the pseudo-second-order kinetics.

The concentration dependence of the rate of sorption was frequently used to analyze the nature of the 'rate-controlling step', and the use of the intra particle diffusion model has been greatly explored in this regard, as represented by Eq. (6), to elucidate its mechanism (Weber and Morris, 1963):

$$q_t = k_{id} t^{1/2} + C \qquad \text{eq. (6)}$$

q_t (mg g^{-1}) is the amount of ammonium ions adsorbed at time *t*, C is the intercept, and k_{id} (mg gmin$^{-0.5}$) is the intra particle diffusion rate constant.

Characterization of biomass

Fourier transform infrared spectroscopy (FT-IR) analysis was also performed on algal biomass before and after ammonium biosorption experiment, using a FT-IR spectrophotometer (Themo 870-FT-IR, Japan), to identify the functional groups possibly involved in the ammonium biosorption. The morphological changes of the algal biomass surface before and after biosorption were obtained using a scanning electron microscope (SEM-S4160, HIACH, Japan)

Results

Fitting the process model

The experimental design matrix for real and coded values along with the observed and predicted values for removal efficiency (%) of ammonium by *G. persica* biomass showen in Table 1. The maximum ammonium ion removal efficiency (%) were found to be 100.01 % in run 7.

Table 1: Box–Behnken design matrix of real and coded values with experimental and predicted values for removal efficiency (%) of ammonium by dried *Gracilaria persica* biomass.

Run order	Real (Coded) values			Removal efficiency (%)	
	X_1	X_2	X_3	Experimental	Predicted
1	0.5 (-1)	6 (0)	1.5 (+1)	67.89	67.17
2	3.5 (+1)	3 (-1)	1 (0)	96.24	96.88
3	0.5 (-1)	9 (+1)	1 (0)	85.99	85.35
4	3.5 (+1)	6 (0)	1.5 (+1)	84.91	84.61
5	2 (0)	6 (0)	1 (0)	98.72	97.24
6	0.5 (-1)	3 (-1)	1 (0)	81.55	82.60
7	3.5 (+1)	6 (0)	0.5 (-1)	100.01	100.73
8	2 (0)	3 (-1)	1.5 (+1)	65.76	65.42
9	2 (0)	6 (0)	1 (0)	97.02	97.24
10	2 (0)	6 (0)	1 (0)	98.99	97.24
11	2 (0)	3 (-1)	0.5 (-1)	85.34	83.98
12	2 (0)	6 (0)	1 (0)	95.13	97.24
13	2 (0)	6 (0)	1 (0)	96.21	97.24
14	2 (0)	9 (+1)	0.5 (-1)	87.11	87.45
15	2 (0)	6 (0)	1 (0)	97.34	97.24
16	0.5 (-1)	6 (0)	0.5 (-1)	92.59	92.89
17	3.5 (+1)	9 (+1)	1 (0)	97.39	96.34
18	2 (0)	9 (+1)	1.5 (+1)	62.81	64.17

X_1: Ammonium concentration (mg L^{-1}); X_2: Initial pH; X_3; Biomass dosage (g L^{-1}).

The calculated regression equation for the optimization of medium constituents showed that the percentage removal of ammonium (Y) was correlated with the function of ammonium concentration (X_1), initial solution pH (X_2) and biomass dosage (X_3). For the three factors studied, the Box-Behnken model could efficiently design quadratic response fit for the surface. In addition, batch mode experiments were carried out with different combinations of the parameters in order to evaluate the combined effects of these factors. As shown in Table 2, the

quadratic model was found to be the most suitable among the four analyzed models. The tests for the significance of regression model were evaluated. The results of the analysis of variance are presented in Table

3. Probability of F less than 0.0001 indicated that the model was significant under selected conditions.

Table 2: Different models for removal (%) of ammonium by dried *Gracilaria persica* biomass.

Source	Sequential F-value	Sequential p-value	Lack of fit p-value	Standard division	R^2	Adjusted R^2	Predicted R^2
Linear	4.5010	0.0207	0.0001	9.41	0.4910	0.3819	0.1321
2FI	0.0949	0.9613	< 0.0001	10.49	0.5038	0.2332	-0.7353
Quadratic	167.3333	< 0.0001	0.3835	1.54	0.9922	0.9835	0.9401
Cubic	1.2549	0.3835		1.47	0.9956	0.9849	

The second order quadratic equation was used to predict the maximum percentage removal of ammonium by dried *G. persica* biomass. The estimated coefficients of equation have been depicted in Table 3. The predicted R^2 value, which was 0.9401 for biosorbent, was in an acceptable agreement with the adjusted R^2 (Table 2).

The adequate precision value was the signal to noise ratio. The ratio of 31.85 for ammonium ions sorption by *G. persica* indicated an adequate signal. The low values of coefficient variation (1.74 %) and Standard Deviation (1.54) showed high reliability.

Table 3: Removal efficiency of ammonium by dried *Gracilaria persica* biomass.

Factor	Coefficient estimate	Standard error	Sum of squares	Mean square	F-value	p-value (probability > F)
Intercept	97.24	0.63				
X_1	6.32	0.54	319.16	319.16	134.56	< 0.0001
X_2	0.55	0.54	2.43	2.43	1.02	0.3410
X_3	-10.46	0.54	875.29	875.29	369.04	< 0.0001
$X_1 X_2$	-0.82	0.77	2.71	2.71	1.14	0.3166
$X_1 X_3$	2.40	0.77	23.04	23.04	9.71	0.0143
$X_2 X_3$	-1.18	0.77	5.57	5.57	2.35	0.1640
X_1^2	2.08	0.74	18.81	18.81	7.93	0.0226
X_2^2	-9.02	0.74	354.93	354.93	149.65	< 0.0001
X_3^2	-12.96	0.74	733.06	733.06	309.08	< 0.0001

DF: Degree of freedom

The minimum value of the standard error design of 0.405 around the centroid also indicated that present model could be used to navigate the design space for the current study (Fig. 1). ANOVA was used for the second order model. The results are given

in Table 3. The significance of each coefficient was determined by F-values and P-values, as listed in Table 3. The larger F-values and the smaller p-values indicated the greater significance of the corresponding coefficients.
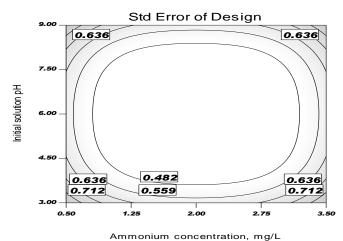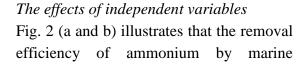
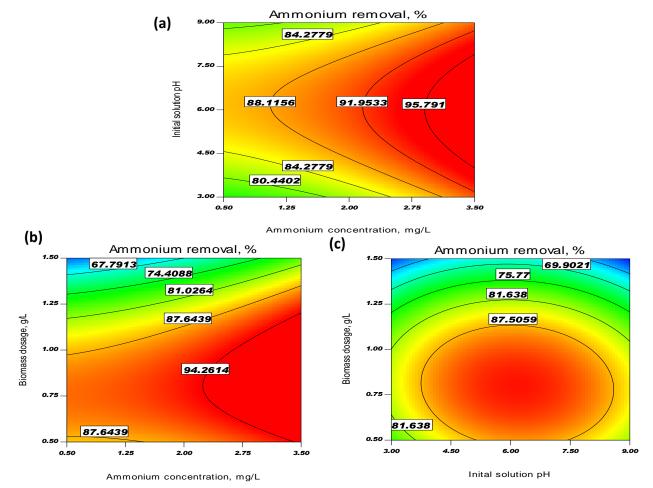**Figure 1: Standard error of design for the model holding ammonium concentration and initial solution pH.**

The effects of independent variables

Fig. 2 (a and b) illustrates that the removal efficiency of ammonium by marine macroalga was increased with an increase in the initial ammonium concentration from 0.5 to 3.5 mg L^{-1}

Figure 2: Counter plots illustrating the interactive effects between ammonium concentration and initial solution pH (a), ammonium concentration and biomass dosage (b) and initial solution pH and biomass dosage (c) on the ammonium removal (%) by dried *Gracilaria persica* biomass.

As shown in Fig. 2 (b and c), removal efficiency of ammonium was increased with an increase in the initial pH of the solution from 3.0 to 6.0, and then ammonium sorption rate was gradually decreased up to 9.0. With increasing the pH, the hydroxyl ions (OH⁻) concentration in the solution was increased, and the surface of alga biomass achieved a negative charge by adsorbing hydroxylions.

Fig. 2 (b and c) represents the interactive effects of biomass dosage (0.5, 1 and 1.5 g L^{-1}) with ammonium concentration and the initial solution pH on the sorption potential of red alga biomass for ammonium removal efficiency. The maximum removal efficiencies of ammonium were acquired from the biomass dosages of 0.82 and 0.79 g L^{-1}, respectively, with the highest ammonium concentration (Fig. 2b) and the middle-level of initial solution pH (Fig 2c).

Independent variables
The perturbation plot was applied to study the influence of three independent factors simultaneously on the ammonium sorption (Fig. 3). The perturbation plot introduced the removal efficiency of ammonium as each variable was moved from the preferred reference, with all other factors being held constant at the coded zero level. As can be seen in this figure, ammonium concentration (A), initial solution pH (B) and biomass dosage (C) were the controlling parameters for achieving the maximum ammonium removal efficiency. A sharp curvature for biomass dosage showed that the response of ammonium removal efficiency was very sensitive to

this factor. The smoother curves for the initial solution pH and ammonium concentration indicated that the sorption of ammonium from the aqueous solution was less effective due to these factors, in comparison to biomass dosage, which was in agreement with coefficient estimates of the regression model, as shown in Table 3.
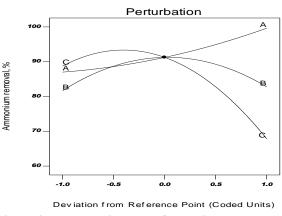

Figure 3: Perturbation plot of three independent variables.

Process optimization for ammonium sorption
In the optimization process, initially one should determine the specific goal for each process variable and their response. The determined goals are combined then into a desirability function. The maximum removal efficiencies of ammonium ions obtained were at an initial solution pH of 6.38, 1 mg L^{-1} of ammonium concentration and the biomass dosage of 0.5 g L^{-1}. At these optimal conditions, the ammonium removal efficiencies predicted were 93.19 %, with the desirability values of 0.9347 (Table 4). Desirability values indicated that the estimated functions could represent the experimental model under the desired conditions.

Table 4: Maximum ammonium removal efficiency by dried *Gracilaria persica* biomass at favorable values of the all experiment variables.

	X_1	X_2	X_3	Ammonium removal (%)	Desirability	
1	1.00	6.38	0.50	93.19	0.9347	Selected
2	1.00	6.28	0.50	93.20	0.9346	
3	1.00	6.4	0.50	93.31	0.9346	
4	1.00	6.42	0.51	93.37	0.9345	
5	1.00	6.25	0.52	93.62	0.9338	

X_1: Ammonium concentration (mg L^{-1}); X_2: Initial pH; X_3; Biomass dosage (g L^{-1}).

Kinetic models

The most used models, including pseudo-first order, pseudo-second order and intra-particle diffusion models, were tested for the adsorption of ammonium ions onto the marine microalga powder. The calculated kinetic parameters and the experimental equilibrium biosorption capacity (mg g^{-1}) at various contact times (0-60 min) are presented in Table 5. The correlation coefficients obtained from the pseudo-second-order model were quite high (R^2=0.99), as compared to those obtained from the pseudo-first-order and intra particle models (R^2=0.84–0.88). The difference between the experimental and predicted values confirmed that the pseudo-first-order model was not appropriate to describe the adsorption kinetics. The plots of q_e versus $t^{1/2}$ were yielded (figures not shown) to determine whether intra particle diffusion was the rate limiting step. As the straight line did not pass through the origin, the intra particle diffusion was not the only rate-controlling factor.

Table 5: Kinetic parameters acquired from pseudo-first-order, pseudo-second-order and intra particle diffusion models of ammonium biosorption by red alga *Gracilaria persica* biomass (T=27 °C, initial pH=6, ammonium concentration=3.5 mg L^{-1}, biomass dosage=0.5 g L^{-1}).

Pseudo-first-order				Pseudo-second-order			Intra particle diffusion		
$k_{1 \times 10}^{1}$ (1 min^{-1})	$q_{e\,exp}$ (mg g^{-1})	q_1 (mg g^{-1})	R^2	$k_{2 \times 10}^{2}$ (mg gmin^{-1})	q_2 (mg g^{-1})	R^2	k_{id} (mg gmin$^{-0.5}$)	C (mg g^{-1})	R^2
0.89	7.01	5.20	0.88	3.97	6.85	0.99	0.39	0.85	0.84

SEM

To get an idea of the microscopic structure of the alga biomass surface and estimate the sorption mechanisms, the surface of *G. persica* before and after ammonium sorption was analyzed through scanning electron microscopy (SEM). As can be seen in Fig. 4, alga surface morphology presented significant differences among the samples. The raw algal cells showed a granular and rough surface morphology. The presence of space between granules played an important role in the adsorption and precipitation of ammonium ions at the external surface. The irregular surface of red macroalga changed to a smooth surface with the obvious cracks and cavities after ammonium sorption.
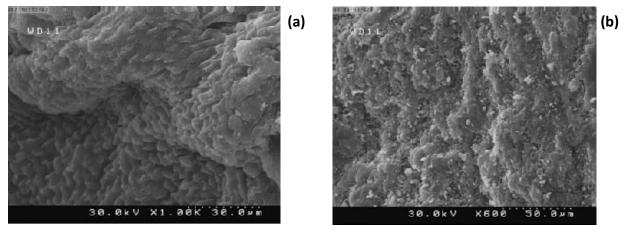
Figure 5: SEM micrograph of red alga *Gracilaria persica* biomass; before (a) and after (b) ammonium biosorption process (T=27 °C, initial solution pH=6, ammonium concentration=1 mg L^{-1}, biomass dosage = 1 g L^{-1}).

FTIR

The FTIR analysis revealed the possible functional groups present in the alga surface. The broad and strong vibration around 3377.56 cm^{-1} confirmed the presence of the −OH and −NH groups. The peak at 2927.70 cm^{-1} demonstrated the presence of −CH stretch. The strong peak at 1654.47 cm^{-1} could be attributed to asymmetric and symmetric stretching vibration of −C=O groups. The weaker band at 1550.09 cm^{-1} was assigned to the presence of C=C band. Association of the peak at 1430.99 cm^{-1} represented the presence of CH_3 group and carboxylate salt COO-M. The bands observed at 1095.59 cm^{-1} were assigned to C–O groups on the alga biomass surface. After ammonium sorption, the bands of 3377, 2927 and 1654 cm^{-1} showed the most variation among other characterized peaks on the alga surface, when these three peaks were shifted to 3453, 2927 and 1636 cm^{-1}.
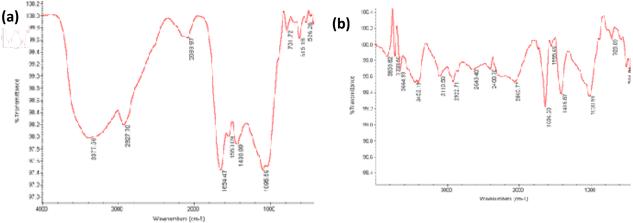

Figure 4: FT-IR spectra of ammonium biosorption by red alga *Gracilaria persica* biomass; before (a) and after (b) ammonium biosorption process (T=27 °C, initial solution pH=6, ammonium concentration = 1 mg L^{-1}, biomass dosage = 1 g L^{-1}).

Discussion

The lack of fit *p*-value of the quadratic model was greater than 0.05 (Table 2) and the non-significant lack-of-fit *p*-value revealed that the selected model was valid for the ammonium biosorption onto red alga *G. persica* biomass (Kousha *et al.,* 2012a). A low probability value

(Probability>F<0.0001) for the quadratic model F-value of 167.33 indicated that the model was significant for ammonium removal by dried *G. persica* biomass

The R^2 and adjusted R^2 values of 0.9922 and 0.9835 for the marine algae biomass were closed to 1, indicating a high correlation between the observed and predicted values (Kousha *et al.,* 2012b).

The predicted residual sum of squares (PRESS) is a measure showing how well the model fits each point in the model (Jabasingh and Pavithra, 2010); the smaller the amount of the PRESS statistic (145.99), the better the model fits the data points. Therefore, the model could be used to navigate the design space.

It was evident that the higher the ammonium concentration led to the higher ammonium removal efficiency of *G. persica* biomass, which was likely due to the increased driving force of the concentration gradient (Khataee and Pourhassan, 2009) as well as the strengthened interaction between ammonium ions and alga biomass (Kousha *et al.,* 2012c). Wahab *et al.* (2010) observed that by increasing the initial ammonium concentration from 10 to 50 mg/L, ammonium sorption capacity onto sawdust was enhanced from 0.56 to 1.26 mg g^{-1} at the temperature of 20 ^{o}C. This finding was in agreement with other reports showing that an increase in ammonium concentration (10-50 mg L^{-1}) resulted in enhancing the sorption capacity of ammonium by cactus leaves fibers (Wahab *et al.,* 2012).

Negatively charged surface onto alga biomass favored the sorption of the cationic ions such as ammonium (NH_4^+) due to electrostatic attraction. Thus, this effect facilitated electrostatic interaction between alga biomass and the positively charged ions (NH_4^+), leading to the maximum ammonium removal. A similar trend was nearly observed for ammonium sorption onto cactus leaves fibers, where ammonium sorption capacity of the plant was increased with the initial solution pH from 3 to 6, and then remained constant up to 10 (Wahab *et al.,* 2012). The maximum ammonium sorption capacity for adsorbents such as sawdust (Wahab *et al.,* 2010), fly ash and sepolite (Ugurlu and Karaoglu, 2011) was eight, which was likely due to the different structure of these adsorbents in relation to plant bio-sorbents.

As can be seen from these figures, increasing the biomass dosage firstly provided greater surface area and ensured the availability of more ammonium ions binding sites. The biomass particle aggregation in higher biomass dosage resulted in the increase of diffusional path length and a sharp decrease in the total surface area of the bio-sorbent and the removal efficiency of ammonium by *G. persica* biomass (Khataee and Pourhassan, 2009). This observation was in agreement with previous the reports showing that malachite green (MG) ions were sorbed by *Senedesmus quadricauda* and *Chlorella vulgaris*. The MG removal efficiency was first increased with an increase in biosorbents dosages from 40 to 80 mg L^{-1}, and then the sorption of MG was decreased with the increase of the bio-sorbents amounts up to 120 mg L^{-1} (Kousha *et al.,* 2013).

A multiple response method was applied for the optimization of any combination of four goals, namely, ammonium

concentration, initial solution pH, biomass dosage of algae, and removal efficiency of ammonium. The goal for the ammonium sorption was to define the sorption process for minimizing biomass dosage, ammonium concentration of 1 mg L^{-1} (based on water quality criteria for cold-water fish (Timmons and Center, 2002), and initial solution pH in the range of 3.0 to 9.0, for maximizing the ammonium removal efficiency in the desirability function.

The pseudo-second order model generated the best fit (R^2=0.99) for the adsorption systems. The sorption capacities (q^2) estimated by the model (6.85 mg g^{-1}) were also close to those acquired by experiments (7.01 mg g^{-1}). These findings suggested that the pseudo-second order was the predominant kinetic model for the kinetics of ammonium ions adsorption onto *G. persica* biomass. The best fit to the this kinetic implied that the rate limiting step of the sorption process could be chemisorption's involving valence forces through sharing or exchange of electrons (Chowdhury *et al.,* 2011).

The results showed that the sorption process was complex and involved more than one mechanism. The calculated parameters are presented in Table 5. The R^2 value was 0.84. Generally, it could be stated that the sorption process tended to follow the intra-particle diffusion (Deniz and Karaman, 2011).

The significant changes in the wave numbers of these specific peaks suggested that amido, aliphatic and carbonyl groups could be involved in the sorption of ammonium ions by *G. persica* biomass

(Sarı and Tuzen, 2008; Esmaeili and Beni, 2015).

In Conclusions, the removal conditions of the ammonium by dried *G. persica* biomass were optimized using Box-Behnken design. The effect of different key parameters including biomass dosage, ammonium concentration and initial solution pH were studied for the ammonium removal by *G. persica*. The maximum ammonium removal efficiency obtained was 100.01%. Different kinetic models were examined, and the pseudo-second order model was selected as the best one to fit the sorption kinetics data. FTIR analysis confirmed the responsibility of different functional groups on the surface of dried *G. persica* biomass for the sorption of ammonium.

The morphological changes of the alga biomass surface were clearly shown in this process using SEM micrographs. The results of the present study suggested that the use of dried *G. persica* biomass could be a good alternative to the current expensive conventional methods used for removing harmful pollutants from wastewater.

References

Chowdhury, S., Chakraborty, S. and Saha, P., 2011. Biosorption of Basic Green 4 from aqueous solution by *Ananas comosus* (pineapple) leaf powder. *Colloids and Surfaces B: Biointerfaces,* 84**,** 520-527.

Davis, T.A., Volesky, B. and Mucci, A., 2003. A review of the biochemistry of heavy metal biosorption by brown algae. *Water Research,* 37**,** 4311-4330.

Deniz, F. and Karaman, S., 2011. Removal of Basic Red 46 dye from aqueous solution by pine tree leaves. *Chemical Engineering Journal,* 170**,** 67-74.

Deniz, F. and Saygideger, S.D., 2011. Removal of a hazardous azo dye (Basic Red 46) from aqueous solution by princess tree leaf. *Desalination,* 268**,** 6-11.

Esmaeili, A. and Beni, A.A., 2015. Biosorption of nickel and cobalt from plant effluent by *Sargassum glaucescens* nanoparticles at new membrane reactor. *International Journal of Environmental Science and Technology,* 12**,** 2055-2064.

Fan, H., Yang, J., Gao, T. and Yuan, H., 2012. Removal of a low-molecular basic dye (Azure Blue) from aqueous solutions by a native biomass of a newly isolated *Cladosporium* sp.: kinetics, equilibrium and biosorption simulation. *Journal of the Taiwan Institute of Chemical Engineers,* 43**,** 386-392.

Galloway, J.N., Dentener, F.J., Capone, D.G., Boyer, E.W., Howarth, R.W., Seitzinger, S.P., Asner, G.P., Cleveland, C., Green, P. and Holland, E., 2004. Nitrogen cycles: Past, present, and future. *Biogeochemistry,* 70**,** 153-226.

Ho, Y.-S. and McKay, G., 1999. Pseudo-second order model for sorption processes. *Process Biochemistry,* 34**,** 451-465.

Jabasingh, S.A. and Pavithra, G., 2010. Response surface approach for the biosorption of Cr^{6+} ions by Mucor racemosus. *CLEAN–Soil, Air, Water,* 38**,** 492-499.

Khataee, A. R. and Pourhassan, M., 2009. Biological decolorization of C.I. basic green 4 solution by *Chlorella* sp.: effect of operational parameters. *Chinese Journal of Applied Environmental Biology,* 15**,** 110-114.

Kismir, Y. and Aroguz, A.Z., 2011. Adsorption characteristics of the hazardous dye Brilliant Green on Saklıkent mud. *Chemical Engineering Journal,* 172**,** 199-206.

Kousha, M., Daneshvar, E., Dopeikar, H., Taghavi, D. and Bhatnagar, A., 2012a. Box–Behnken design optimization of Acid Black 1 dye biosorption by different brown macroalgae. *Chemical Engineering Journal,* 179**,** 158-168.

Kousha, M., Daneshvar, E., Esmaeli, A. R., Jokar, M. and Khataee, A.R., 2012b. Optimization of Acid Blue 25 removal from aqueous solutions by raw, esterified and protonated *Jania adhaerens* biomass. *International Biodeterioration and Biodegradation,* 69**,** 97-105.

Kousha, M., Daneshvar, E., Sohrabi, M. S., Jokar, M. and Bhatnagar, A., 2012c. Adsorption of acid orange II dye by raw and chemically modified brown macroalga *Stoechospermum marginatum*. *Chemical Engineering Journal,* 192**,** 67-76.

Kousha, M., Farhadian, O., Dorafshan, S., Soofiani, N.M. and Bhatnagar, A., 2013. Optimization of malachite green biosorption by green microalgae—

Scenedesmus quadricauda and *Chlorella vulgaris*: application of response surface methodology. *Journal of the Taiwan Institute of Chemical Engineers,* 44**,** 291-294.

Lagergren, S., 1898. Zur theorie der sogenannten adsorption geloster stöffe, Kungliga Sevenska Vetenskapsakademiens. Handlingar. 24 P.

Liu, H., Dong, Y., Wang, H. and Liu, Y., 2010. Ammonium adsorption from aqueous solutions by strawberry leaf powder: Equilibrium, kinetics and effects of coexisting ions. *Desalination,* 263**,** 70-75.

Neal, C. and Heathwaite, A. L., 2005. Nutrient mobility within river basins: a European perspective. *Journal of Hydrology,* 304**,** 477-490.

Rice, E.W., Bridgewater, L. and Association, A.P.H., 1999. Standard methods for the examination of water and wastewater, American Public Health Association Washington, DC. 2671 P.

Sarı, A. and Tuzen, M., 2008. Biosorption of total chromium from aqueous solution by red algae (*Ceramium virgatum*): Equilibrium, kinetic and thermodynamic studies. *Journal of Hazardous Materials,* 160**,** 349-355.

Timmons, M.B. and Center, N.R.A., 2002. Recirculating aquaculture systems. 948 P.

Ugurlu, M. and Karaoglu, M.H., 2011. Adsorption of ammonium from an aqueous solution by fly ash and sepiolite: isotherm, kinetic and thermodynamic analysis. *Microporous and Mesoporous Materials,* 139**,** 173-178.

Wahab, M. A., Jellali, S. and Jedidi, N., 2010. Ammonium biosorption onto sawdust: FTIR analysis, kinetics and adsorption isotherms modeling. *Bioresource Technology,* 101**,** 5070-5075.

Wahab, M. A., Boubakri, H., Jellali, S. and Jedidi, N., 2012. Characterization of ammonium retention processes onto cactus leaves fibers using FTIR, EDX and SEM analysis. *Journal of Hazardous Materials,* 241**,** 101-109.

Weber, W.J. and Morris, J.C., 1963. Kinetics of adsorption on carbon from solution. *Journal of the Sanitary Engineering Division,* 89**,** 31–59.

Zheng, H., Han, L., Ma, H., Zheng, Y., Zhang, H., Liu, D. and Liang, S., 2008. Adsorption characteristics of ammonium ion by zeolite 13X. *Journal of Hazardous Materials,* 158**,** 577-584.